Surface treatment on polyethylenimine interlayer to improve inverted OLED performance*

Chang-Ting Wei(魏昌庭)[1,2], Jin-Yong Zhuang(庄锦勇)[2], Ya-Li Chen(陈雅丽)[1,†]
Dong-Yu Zhang(张东煜)[2,‡], Wen-Ming Su(苏文明)[2], and Zheng Cui(崔铮)[2]

[1] *Department of Chemistry, Shanghai University, Shanghai* 200444, *China*
[2] *Printable Electronics Research Center, Suzhou Institute of Nano-Tech and Nano-Bionics, Chinese Academy of Sciences, Suzhou* 215123, *China*

(Received 11 March 2016; revised manuscript received 12 June 2016; published online 25 August 2016)

Polyethylenimine (PEI) interlayer rinsing with different solvents for inverted organic light emitting diodes (OLEDs) is systematically studied in this paper. In comparison with the pristine one, the maximum current efficiency (CE_{max}) and power efficiency (PE_{max}) are enhanced by 21% and 22% for the device rinsing by ethylene glycol monomethyl ether (EEA). Little effect is found on the work function of the PEI interlayer rinsed by deionized water (DI), ethanol (EtOH), and EEA. On the other hand, the surface morphologies of PEI through different solvent treatments are quite different. Our results indicates that the surface morphology is the key to improving the device performance for IOLED as the work function of PEI keeps stable.

Keywords: inverted OLED, surface treatment, morphology, polyethylenimine

PACS: 85.60.Jb, 78.60.Fi, 72.80.Le **DOI:** 10.1088/1674-1056/25/10/108505

1. Introduction

Over the past decades, organic light emitting diodes (OLEDs) have attracted a great deal of attention due to their intriguing applications in full-color display and solid-state lighting since the pioneering work of Tang and VanSlyke.[1–8] Recently, active matrix organic light emitting diode (AMOLED) display as a new-generation all-solid technology has been widely employed in smart phones, tablet personal computers (PCs), digital cameras, large-size televisions (TVs), and flexible wearable devices due to its high performance and low cost.[9–12] It is well known that the performance (particularly the stability and uniformity) of the thin-film transistor (TFT) in each AMOLED pixel is vital to achieving full color displays.[9,13] Generally, the oxide TFT backplane is adapted to the commercial AMOLED backplane due to its better uniformity, lower processing temperature, higher carrier mobility, higher transparency, and potentially better electrical stability than the low-temperature polycrystalline silicon TFT and amorphous silicon TFT backplane. The inverted OLED (IOLED) structure with bottom cathode is superior to the conventional OLED structure on account of the oxide TFT backplane possessing the n-type transistor characteristics. Simultaneously, the bottom cathode and n-type drain can be connected directly in IOLED structure, which can increase the stability and reduce the driving voltage.[14] In addition, the conventional structure of bottom-emitting OLED (IBOLED) device generally use indium tin oxide (ITO) as a transparent anode, in which the aperture ratio is only in a range from 30% to 50%. In contrast, the inverted (IOLED) device has a larger aperture ratio, higher stability, longer lifetime, and fewer image sticking phenomena than the conventional OLED.[9,13–15]

Solution-processing for OLED fabrication has been developed rapidly for its low cost, large scale manufacturing and large-size OLED displays.[16–19] As is well known, ITO is widely used as the anode for its high work function of about 4.8 eV, when used as the cathode, a 1.6–2.0 eV injection barrier exists between the lowest unoccupied molecular orbital (LUMO) level of the electron transport material (ETM) and that of the cathode. Therefore, the development of suitable solution method for processing electron injection materials is essential. It has been reported that by using the zinc oxide (ZnO) nanoparticles (NPs), the work function of ITO/ZnO can be tuned from 4.8 eV to 4.1 eV. However, there still exists an injection barrier between the organic layer and ZnO.[20] In order to solve this problem, Zhou *et al.* reported that introducing polyethyleneimine (PEI) between the metal oxides (such as ITO, ZnO), the organic layer can significantly improve the device performance.[21] The thin film layer of PEI will form interface dipoles and lower the work function. Since then, PEI has been used as an effective electron-injecting layer in inverted devices both for OLEDs and quantum dots light emitting diodes(QDLEDs).[22–27] In 2014, Höfle *et al.* reported the deposition of PEI on the ZnO as a combined interlayer in

*Project supported by the National Key Basic Research Project of China (Grant No. 2015CB351901), the Strategic Priority Research Program of the Chinese Academy of Sciences (Grant No. XDA09020201), the Youth Innovation Promotion Association of Chinese Academy of Sciences (Grant No. 2013206), the National Natural Science Foundation of China (Grant No. 21402233), and the Natural Science Foundation of Jiangsu Province, China (Grant Nos. BK2012631 and BK20140387).

†Corresponding author. E-mail: ylchen@staff.shu.edu.cn
‡Corresponding author. E-mail: dyzhang2010@sinano.ac.cn

© 2016 Chinese Physical Society and IOP Publishing Ltd

an inverted polymer light-emitting diode, which can enhance the electron injection from the cathode into the emitting layer (EML). It has been reported that the PEI film was rinsed with water or ethanol to remove PEI surplus, though there is not any relevant mechanism described yet.[28,29]

In this paper, the properties of PEI layer treated with deionized water (DI), ethanol (EtOH) and ethylene glycol monomethyl ether (EEA) are systematically investigated. The work function and surface morphology of PEI are measured. Our work indicates that the solvent rinsing has little effect on the work function. On the other hand, the surface morphology of PEI is quite different from various solvent treatments. The electroluminescent properties of both fluorescent and phosphorescent OLEDs based on PEI are characterized. A maximum current efficiency and power efficiency (PE_{max}) of EEA treated phosphorescent devices (CE_{max}) reach 30.54 cd·A^{-1} and 13.90 lm·W^{-1}, respectively, which are increased by 21% and 22% compared with that of the untreated one. Based on the investigations of the PEI layer, the significant device improvement can be attributed to better interlayer contact with the neighboring organic layer.

2. Experiment

2.1. Materials

All chemicals and reagents were used as received from commercial sources without further purification. PEI (M_w = 25000 g/mol) was purchased from Sigma-Aldrich. EtOH was of analytically pure grade from Sinopharm Chemical Reagent Co., Ltd. (China), EEA was of analytically pure grade from Sigma-Aldrich (USA). DI with resistance of 18 MΩ·cm@25 °C used all through the experiment was purified by Direct-Q5uv manufactured by Merck Millipore. Alq_3, $Ir(ppy)_3$, 4,4-bis(9-carba-zolyl)-2,2-biphenyl(CBP), [N-(1-naphthy1)-npheny1-amino] biphenyl (NPB) and 1-bis [(di-4-tolylamino) phenyl]cyclohexane (TAPC) were purchased from Nichem Fine Technology Co. Ltd. MoO_3 was purchased from Alfa Aesar. ZnO NPs were synthesized according to the previously reported procedures, and were dispersed in acetone with a concentration of 10 mg·mL^{-1} prior to use.[30]

2.2. General information

The film surface morphology was measured with Veeco Dimension 3100 (USA) at ambient temperature in a tapping mode. The work function was measured on the Veeco Dimension 3100 Kelvin probe force microscope (USA) at ambient temperature. Highly ordered pyrolytic graphite, whose work function in air is 4.6 eV, was taken as the reference. The thickness values of solution-processed films were measured using an AlphaStep profilometer (Veeco, Dektak150). All electrical testing measurements were performed under ambient conditions without further encapsulation. The electroluminescent spectra were measured with a Spectra Scan PR655. The current–voltage (I–V) and luminance–voltage (L–V) characteristics were measured with a computer controlled Keithley 2400 Sourcemeter. The active area of the device was 2 mm×2 mm, and only the luminance in the forward direction was measured.

2.3. Device fabrication of IOLED devices

The chemical structures, device configurations, and the energy level diagrams of IOLEDs with the PEI rinsing with EEA are shown in Fig. 1 and Fig. 2. OLEDs were fabricated on an ITO substrate with a sheet resistance of ∼ 20 Ω/sq. Prior to use, the ITO substrate was degreased with solvents and treated with O_2-plasma for 3 min. First, a 30-nm ZnO layer was deposited by spin-coating (2300 rpm for 60 s) on a pre-cleaned ITO substrate and then baked at 120 °C for 10 min in the glove box. The PEI was dissolved in EEA with a concentration of 0.4 wt% and spin-coated at 5000 rpm for 50 s onto the ZnO layer.[28] After the coating of PEI, the substrate was baked at 100 °C for 10 min to remove residual solvent. The resulting solvents, including DI (in air), EtOH (in N_2) and the EEA (in N_2), were spin-coated on PEI film after annealing, at 2000 rpm for 60 s and then dried at 100 °C for 10 min in nitrogen atmosphere. Then the samples were directly loaded into the evaporation system. After the deposition of PEI, the EML of Alq_3 (70 nm), a hole-transporting layer (HTL) of NPB (30 nm), a hole-injection layer (HIL) of MoO_3 (10 nm) and Al were deposited layer by layer in the vacuum of 5×10^{-4} Pa. As for the green phosphorescent device, the EML consists of CBP and $Ir(ppy)_3$(8%, 40 nm), and TAPC (30 nm) as the HTL.

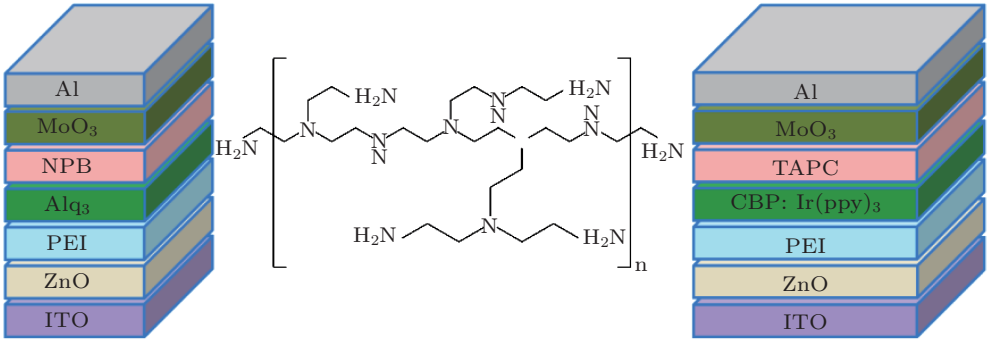


Fig. 1. (color online) Chemical structures of PEI and the IOLEDs structures based on Alq_3 and $Ir(ppy)_3$ as EML.

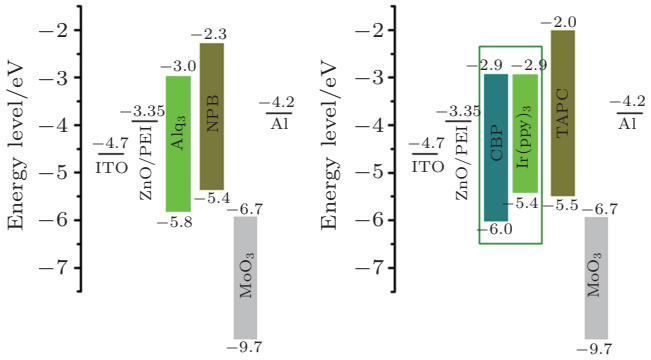


Fig. 2. (color online) Energy level diagrams of (a) Alq_3, (b) $Ir(ppy)_3$ IOLEDs with the PEI rinsing with EEA.

3. Results and discussion

Since the PEI layer is rinsed by different solvents, the work function and film mophology are investigated. The thickness of untreated PEI film is about 10 nm, then decreases to 8 nm after being treated by solvent, which is in accordance with the reported result.[22] Firstly, the work functions of ZnO/PEI with different-solvent surface treatment were performed by Kelvin probe force microscopy (KFM). As shown in Table 1, the work function values of ZnO/PEI rinsed with DI, EtOH, and EEA are 3.40, 3.37, and 3.35 eV, respectively, in comparison with 3.50 eV of the untreated (W/O) one. As a result, the work function of ZnO/PEI is slightly affected by the solvent treatment.

As is well known, the film morphology is very important for the device performance. Here, the film forming properties of PEI are investigated by AFM. Figure 3 shows the AFM images of PEI film surfaces treated with W/O (Fig. 3(a)) and with (Fig. 3(b)) DI, (Fig. 3(c)) EtOH, and (Fig. 3(d)) EEA. As shown in Table 1, the values of surface roughness (R_a) of PEI film W/O rinsed with DI, EtOH, and EEA are 4.12, 4.35, 2.76, 2.65 nm, respectively. These results imply that the different treatments have different influences on the film-forming properties of PEI. In Fig. 3, there are a lot of "island" bulges for the PEI layer treated by DI. As for the PEI treated with EtOH and EEA, the surface roughness and film uniformity are significantly improved compared with the W/O one. As a result, the physical contact between PEI and EML becomes more efficient, and better device performance can be expected. The physical properties of DI, EtOH, and EEA are compared further and find that the main difference among them consists in polarity value and boiling point. The polar values and the boiling points of DI, EtOH, and EEA are 10.2, 4.3, 5.0,[31] 100 °C, and 78 °C, 135 °C, respectively. From these data, it is possible that the differences in solvent polarity and boiling point have a direct influence on the film-forming state of PEI, leading to the different performances of devices.[26,32–34]

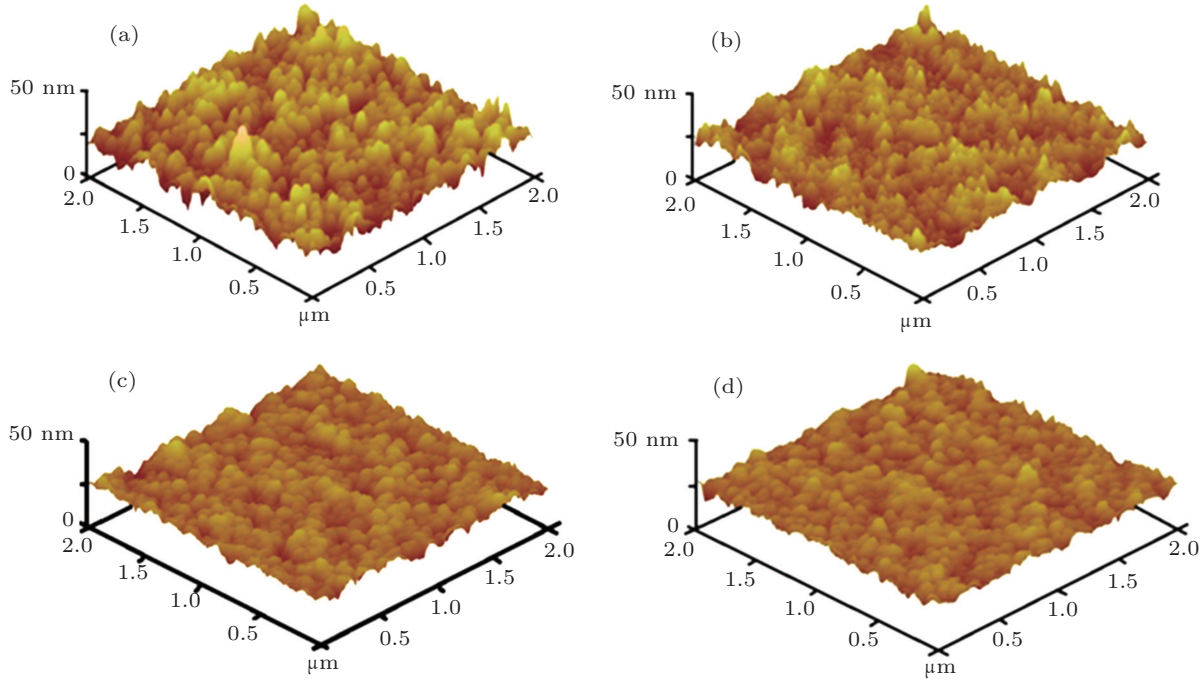


Fig. 3. (color online) AFM topographic images (2 μm ×2 μm) of the PEI surface W/O (a) and with (b) DI, (c) EtOH, and (d) EEA treatment.

Table 1. Values of work function and surface roughness of ZnO/PEI with different-solvent surface treatment.

Solvent	W/O	DI	EtOH	EEA
Work function/eV	3.50	3.40	3.37	3.35
Surface roughness (R_a)	4.12	4.35	2.76	2.65

In other words, the PEI layer experiences the EtOH and EEA treatment, some agglomeration particles and interface defects can be removed, thereby the ability to inject the electrons from ILs to EML is improved. But in the case of the DI

treated one, the interface defects are actually increased, then the ability to inject and tranport the electrons is reduced, eventually leading to the lowest device performance.[26,32–34]

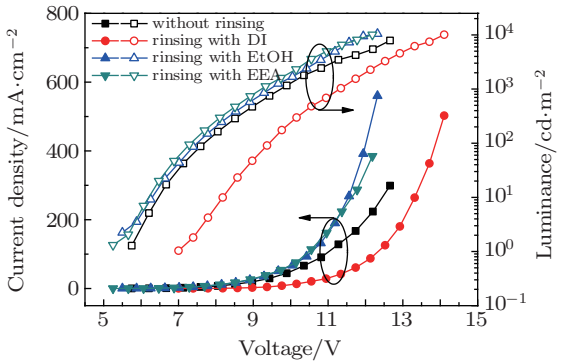


Fig. 4. (color online) *J–V–L* characteristics of Alq_3 IOLEDs with different surface treatment processes on the PEI layer.

The current density–voltage–luminance (*J–V–L*) and the current efficiency–luminance–power efficiency (*CE–L–PE*) characteristics of the fluorescent IOLEDs are shown in Figs. 4 and 5, respectively. It is obious that both the current density and luminance for the device treated with DI are significantly lower than those of the device without rinsing. As for devices treated with EtOH and EEA, both current density and brightness are significantly enhanced at the same voltage. As shown in Table 2, the turn-on voltage (V_{on}), the maximum luminance (L_{max}), CE_{max}, PE_{max} and the maximum external quantum efficiency (EQE_{max}) of the optimized EEA treated device are 5.2 V, 10090 cd·m^{-2}, 3.16 cd·A^{-1}, 0.98 lm·W^{-1}, and 1.05%, in contrast to the untreated one, the turn-on voltage is reduced by 0.4 V, the L_{max}, CE_{max}, PE_{max}, and EQE_{max} are increased by 28%, 17%, 21%, and 18%, respectively. In other words, EEA treatment improves the injection and the balance of the carrier in the device. From the electroluminescent (EL) spectra of the devices as shown in the inset of Fig. 6, all EL spectra are completely overlapped, indicating that the treatment only changes the interface contact beween the EML and ILs, so there is no side effect on the properties of emitting material. This is very valuable for fabricateing the solution preparation multilayer device.

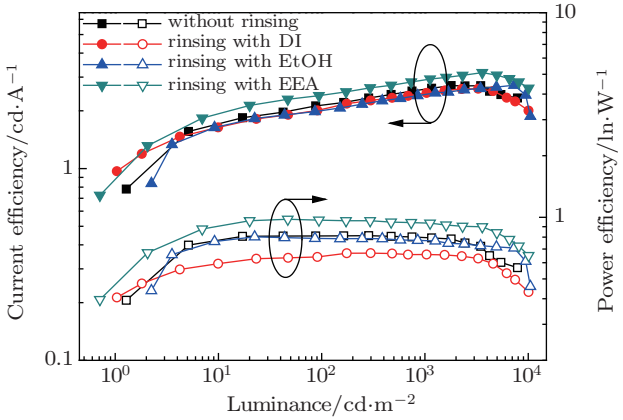


Fig. 5. (color online) *CE–L–PE* characteristics of Alq_3 IOLEDs with different surface treatment processes on PEI layer.

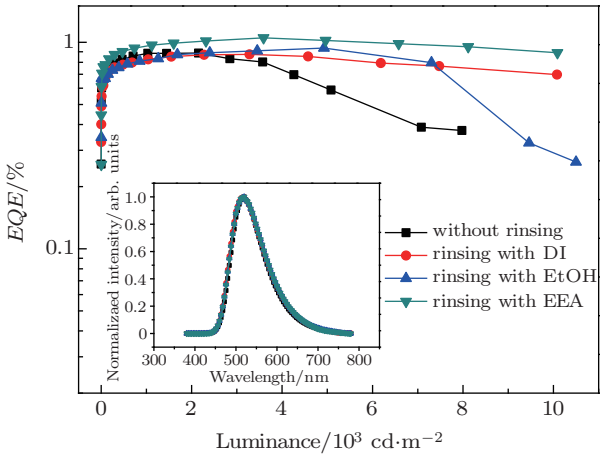


Fig. 6. (color online) *EQE–V* (Inset: EL spectra.) characteristics of Alq_3 IOLEDs with different surface treatment processes on PEI layer.

Table 2. Device performances of IOLEDs with different-solvent surface treatment.

Devices	V_{on}/V (1 cd·m^{-2})	Luminance/cd·m^{-2}	*CE*/cd·A^{-1} Maximum	*PE*/lm·W^{-1}	*EQE*/%
Without rinsing	5.6	7873	2.71	0.81	0.89
Rinsing with DI	7.0	10080	2.61	0.67	0.87
Rinsing with EtOH	5.4	10050	2.72	0.80	0.94
Rinsing with EEA	5.2	10090	3.16	0.98	1.05

For studing the universality of surface treatment method on PEI, we apply it to an $Ir(ppy)_3$ green phosphorescent device. The *J–V–L* and the *CE–L–PE* characteristics of the $Ir(ppy)_3$ IOLEDs are shown in Figs. 7 and 8, respectively. In accordance with the results in the above-mentioned Alq_3 IOLEDs, compared with those in the W/O $Ir(ppy)_3$ IOLEDs, the performance of EtOH and EEA treated devices are significantly improved too. As shown in Table 3, the values of V_{on}, L_{max}, CE_{max}, PE_{max}, and EQE_{max} of the optimized EEA treated device are 5.1 V, 18830 cd·m^{-2}, 30.54 cd·A^{-1}, 13.90 lm·W^{-1}, and 8.95%, respectively. The turn-on voltage is reduced by 0.6 V, the L_{max}, CE_{max}, PE_{max}, and EQE_{max} are increased by 36%, 21%, 22%, and 20% compared with those of the W/O one, respectively. On the contrary, the turn-on voltage and the L_{max} of the DI treated device are 7 V and 6216 cd·m^{-2}, which are significantly inferior to those of the

W/O one. From the EL spectra of the devices with and without being treated as shown in the inset of Fig. 9, we can find that all EL spectra are completely overlapped, indicating that the solvent surface treatment does not spoil the phosphorescent emitting material. It proves again that EEA treatment has potential applications in the solution process multilayer phosphorescent devices.

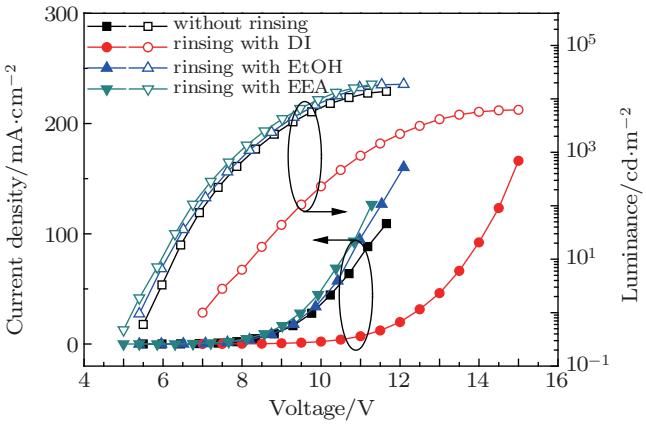


Fig. 7. (color online) *J–V–L* characteristics of Ir(ppy)$_3$ IOLEDs with different surface treatment processes on PEI layer.

We suggest that the improved device performance of the EEA treated phosphorescent device also results from the optimizing of morphology and the suppressed interface defect states on PEI surface as mentioned earlier.[26,32–34] In addition, from Table 3, it is noteworthy that the EQE of the optimized device only drops about 26.34% when the brightness is increased from the 1000 cd·m^{-2} to 10000 cd·m^{-2}, while that of the W/O one drops about 32.22%. The *EQE* roll–off, furthermore the stability of EEA treated phosphorescent device, are significantly improved. In contrast, the DI treated device, its carrier injection and transmission are deteriorated due to the increased interface defects and bad interface contact, which results in the inferior device performance.

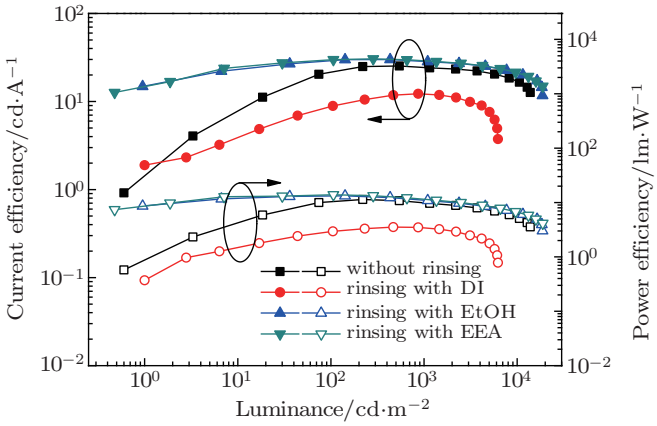


Fig. 8. (color online) *CE–L–PE* characteristics of Ir(ppy)$_3$ IOLEDs with different surface treatment processes on PEI layer.

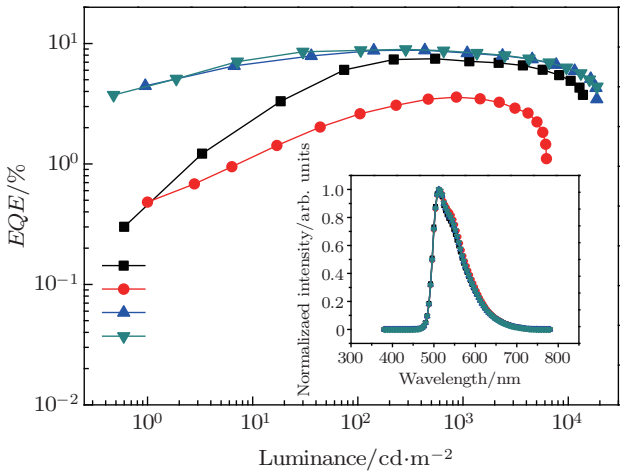


Fig. 9. (color online) *EQE–V* (Inset: EL spectra.) characteristics of Ir(ppy)$_3$ OLEDs with different surface treatment processes on PEI layer.

Table 3. Device performances of phosphorescent IOLEDs with different-solvent surface treatment.

Devices	V_{on}/V (1 cd·m^{-2})	Luminance/cd·m^{-2}	*CE*/cd·A^{-1} Maximum	*PE*/lm·W^{-1}	*EQE*/%	*EQE* roll-off/% 10^3–10^4 cd·m^{-2}
Without rinsing	5.7	13820	25.33	11.37	7.47	32.22
Rinsing with DI	7.0	6216	12.24	3.53	3.58	–
Rinsing with EtOH	5.4	18710	29.95	13.26	8.79	26.50
Rinsing with EEA	5.1	18830	30.54	13.90	8.95	26.34

4. Conclusions

In this work, we systematically investigate the effects of PEI injection layer rinsed with different polar solvents, including DI, EtOH, and EEA. Our work indicates that there are slight effects on the work function of PEI rinsed with these different solvents, but a big influence is exerted on the surface morphology. The EEA treatment can effectively lower the surface roughness, reduce the interfacial defects and improve the physical contact between ILs and the EML. Both the fluorescent and phosphorescent OLEDs based on the PEI rinsed with EEA achieve the best device performances. A maximum current efficiency (CE_{max}) and power efficiency (PE_{max}) are enhanced by 21% and 22% for the phosphorescent OLEDs. Our work indicates that the solution-processed OLED performance can be achieved by simple solvent treatment.

References

[1] Tang C W and VanSlyke S A 1987 *Appl. Phys. Lett.* **51** 913
[2] Burroughes J, Bradley D, Brown A, Marks R, Mackay K, Friend R, Burns P and Holmes A 1990 *Nature* **347** 539
[3] Baldo M A, O'brien D, You Y, Shoustikov A, Sibley S, Thompson M and Forrest S 1998 *Nature* **395** 151

[4] Friend R, Gymer R, Holmes A, Burroughes J, Marks R, Taliani C, Bradley D, Dos Santos D, Bredas J and Lögdlund M 1999 *Nature* **397** 121

[5] Müller C D, Falcou A, Reckefuss N, Rojahn M, Wiederhirn V, Rudati P, Frohne H, Nuyken O, Becker H and Meerholz K 2003 *Nature* **421** 829

[6] Sun Y, Giebink N C, Kanno H, Ma B, Thompson M E and Forrest S R 2006 *Nature* **440** 908

[7] Yu J N, Zhang M Y, Li C, Shang Y Z, Lv Y F Wei B and Huang W 2012 *Chin. Phys. B* **21** 083303

[8] Miao Y Q, Gao Z X, Zhang A Q, Li Y H, Wang H, Jia H S, Liu X G and Tsuboi T 2015 *Chin. Phys. B* **24** 057802

[9] Hsieh H H, Tsai T T, Chang C Y, Wang H H, Huang J Y, Hsu S F, Wu Y C, Tsai T C, Chuang C S and Chang L H 2010 *SID Int. Symp. Dig. Tech. Pap.* **41** 140

[10] Fan Y, Zhang H, Chen J and Ma D 2013 *Org. Electron.* **14** 1898

[11] Shih T H, Ting H C, Lin P L, Chen C L, Tsai L, Chen C Y, Lin L F, Liu C H, Chen C C and Lin H S 2014 *SID Int. Symp. Dig. Tech. Pap.* **45** 766

[12] Song E and Nam H 2014 *Displays* **35** 118

[13] Lee J H, Wang P S, Park H D, Wu C I and Kim J J 2011 *Org. Electron.* **12** 1763

[14] Lee H, Park I, Kwak J, Yoon D Y and Lee C 2010 *Appl. Phys. Lett.* **96** 153306

[15] Chen J, Shi C, Fu Q, Zhao F, Hu Y, Feng Y and Ma D 2012 *J. Mater. Chem.* **22** 5164

[16] Ding Z, Xing R, Fu Q, Ma D and Han Y 2011 *Org. Electron.* **12** 703

[17] Wilson P, Lekakou C and Watts J F 2012 *Org. Electron.* **13** 409

[18] Perelaer J, Abbel R, Wünscher S, Jani R, Van Lammeren T and Schubert U S 2012 *Adv. Mater.* **24** 2620

[19] Coenen M J, Slaats T M, Eggenhuisen T M and Groen P 2015 *Thin Solid Films* **583** 194

[20] Kabra D, Lu L P, Song M H, Snaith H J and Friend R H 2010 *Adv. Mater.* **22** 3194

[21] Zhou Y, Fuentes-Hernandez C, Shim J, Meyer J, Giordano A J, Li H, Winget P, Papadopoulos T, Cheun H and Kim J 2012 *Science* **336** 327

[22] Kim Y H, Han T H, Cho H, Min S Y, Lee C L and Lee T W 2014 *Adv. Funct. Mater.* **24** 3808

[23] Stolz S, Scherer M, Mankel E, Lovrincic R, Schinke J, Kowalsky W, Jaegermann W, Lemmer U, Mechau N and Hernandez-Sosa G 2014 *ACS Appl. Mater. Interfaces* **6** 6616

[24] Min X, Jiang F, Qin F, Li Z, Tong J, Xiong S, Meng W and Zhou Y 2014 *ACS Appl. Mater. Interfaces* **6** 22628

[25] Fan C, Lei Y, Liu Z, Wang R, Lei Y, Li G, Xiong Z and Yang X 2015 *ACS Appl. Mater. Interfaces* **7** 20769

[26] Yan L, Song Y, Zhou Y, Song B and Li Y 2015 *Org. Electron.* **17** 94

[27] Yang W, Liu Z, Chen J, Huang L, Zhang L, Pan H, Wu B and Lin Y 2015 *Sci. Rep.* **5**

[28] Höfle S, Schienle A, Bruns M, Lemmer U and Colsmann A 2014 *Adv. Mater.* **26** 2750

[29] Höfle S, Schienle A, Bernhard C, Bruns M, Lemmer U and Colsmann A 2014 *Adv. Mater.* **26** 5155

[30] Beek W J, Wienk M M, Kemerink M, Yang X and Janssen R A 2005 *J. Phys. Chem. B* **109** 9505

[31] West S D 1987 *J. Chromatogr. Sci.* **25** 122

[32] Liu S, Ho S, Chen Y and So F 2015 *Chem. Mater.* **27** 2532

[33] Dong W F, Liu S, Wan L, Mao G, Kurth D G and Möhwald H 2005 *Chem. Mater.* **17** 4992

[34] Staudigel J, Stößel M, Steuber F and Simmerer J 1999 *J. Appl. Phys.* **86** 3895